Cybersickness-related changes in brain hemodynamics: a pilot study comparing transcranial Doppler and near-infrared spectroscopy assessments during a virtual ride on a roller coaster.

[1]Alireza Mazloumi Gavgani, [1]Rachel HX Wong, [1]Peter RC Howe, [2]Deborah M. Hodgson, [1]*Frederick R Walker, [1]*Eugene Nalivaiko

[1]School of Biomedical Sciences and Pharmacy and [2]School of Psychology, University of Newcastle, Callaghan NSW 2308, Australia

Corresponding author: A/Prof Eugene Nalivaiko
School of Biomedical Sciences and Pharmacy
University of Newcastle
Callaghan NSW 2308, Australia

Tel. +61 2 4921 5620
Email: Eugene.nalivaiko@newcastle.edu.au

* - these authors made equal contribution to the current work.

ABSTRACT

Our aim was to assess cerebral blood flow changes during cybersickness. Transcranial Doppler (TCD) ultrasound and near infrared spectroscopy (NIRS) were used separately in two independent experiments. In both studies, a 15-min virtual roller coaster ride was used as a provocative visual stimulus. Subjective nausea ratings were obtained at 1 min intervals. The TCD study was performed in 14 healthy subjects (8 males and 6 females); in this study we also measured heart rate and arterial pressure. In a separate study a 52-channel NIRS device (Hitachi ETG-4000) was used to monitor activated brain regions by measuring oxy-hemoglobin ($HbO_{2)}$ concentration in 9 healthy subjects (4 male, 5 females). The TCD study results showed a significant increase in systolic (+3.8±1.8 mmHg) and diastolic (+6.7±1.3 mmHg) pressure at the end of the virtual ride (maximum nausea) compared to baseline (no nausea). We also found that middle cerebral artery (MCA) and posterior cerebral artery (PCA) systolic flow velocity decreased significantly at the end of the ride when compared to baseline values. Likewise, the relative systolic and diastolic conductance in the MCA decreased significantly (-0.03±0.02 cm x s^{-1} x $mmHg^{-1}$, t, p=0.0058 and -0.03±0.01 cm x s^{-1} x $mmHg^{-1}$, p=0.05, respectively) at maximum nausea when compared to no nausea. Additionally, there was a significant decrease (-0.02±0.01cm x s^{-1} x $mmHg^{-1}$, p=0.03) in the relative systolic conductance in the PCA at the end of the ride. Analysis of the NIRS results showed a significant increase in HbO_2 concentration in 15/52 channels in parieto-temporal regions of both hemispheres in participants who experienced motion sickness symptoms during the experiment. This increase in HbO_2 concentration correlated with increasing nausea and motion sickness symptoms. We conclude that cybersickness causes complex changes in cerebral blood flow, with an increase in perfusion in some cortical regions, but with a decrease of global cerebral perfusion.

Key words: motion sickness, nausea, virtual reality, cerebral blood flow.

1. INTRODUCTION

Motion sickness (MS) is considered to be a general feeling of discomfort in ordinary routine life but also a major operational hazard for pilots and space agencies. It is currently well accepted that conflicting signals from the spatial orientation senses – visual, vestibular and proprioceptive leads to the development of motion sickness [1]. This sensory conflict which was first described by Irwin [2] and later explained by James [3] in the early 19th century can be a result of single sensory system mismatch such as canal-otolith interaction during Coriolis cross-coupling, or between two or more sensory systems such as visual/vestibular/proprioceptive interference [4]. These early findings suggest that the vestibular system plays a critical role in the pathogenesis of motion sickness [2]. Other research has concluded that subjects with bilateral vestibular deficit are immune to motion sickness [3, 5]; hence the vestibular system is indispensable in evolution of motion sickness. One potential cause of neuronal dysfunction responsible for motion sickness is alteration in regional cerebral blood supply; thus a close investigation of vestibular inputs in the regulation of cerebral blood flow is essential for better understanding the underlying mechanisms associated with motion sickness.

A recent study has found that people who suffer from motion sickness during parabolic flight are more likely to have orthostatic intolerance and increased cerebrovascular resistance after flight [6]. Serrador et al reported an increase in cerebrovascular resistance and decreases in cerebral flow velocity minutes before any motion sickness symptom was experienced in an experiment where subjects were rotated in a human centrifuge [7]. A study by Heckmann [8] found that caloric vestibular stimulation of the semicircular canals increases blood flow in the basilar artery. A similar study utilizing caloric stimulation reported an increase in the middle cerebral artery (MCA) blood flow while a significant decrease was seen in the flow in the posterior cerebral artery (PCA). These researches suggest that cerebral blood flow (CBF) changes with increasing nausea and motion sickness.

There are several methods to assess CBF; in recent studies a link between the neural metabolism and perfusion in the brain has been demonstrated using devices such as single photon emission computed tomography[9], positron emission tomography [10] and the xenon-133 inhalation technique [11]. Transcranial Doppler (TCD) ultrasound is another device that has been widely used as a screening tool in monitoring perfusion in stroke [12-14], trauma [13], screening lesions [15, 16] and other studies concerning the hemodynamic changes in the brain such as MCA blood flow during diverse stimulation maneuvers, viz. cycling, reading and writing [17], or flow alteration in Posterior Cerebral Artery (PCA) [18]. Another technique which is extensively used in observing CBF is near infrared spectroscopy (NIRS). This device

uses the basic concept of emission of near-infrared light (NIR) at the surface of the head and detection of reflected light at a distance of a several centimeters to determine hemoglobin concentration in the cerebral cortex. Due to the non-invasive nature and simple application of the NIRS device, this tool has been utilized in various aspects of brain imaging. Some studies have used this tool to monitor brain injury and ischemic regions in the brain looking at regional cerebral blood flow in brain-injured patients [19], others have employed this tool to screen brain activation regions while performing certain mental [20, 21] and physical [22, 23] tasks. NIRS has been used to closely monitor brain blood flow in other neurogenic diseases such as dementia, Alzheimer's [24], schizophrenia [25] and infant brain studies [26, 27]. Several previous studies have shown close correspondence between fMRI and NIRS signals with significant spatial and temporal correlations [28] [29].

However, the inherent limitation of these screening methods when used in conjunction with physical motion sickness provocation – motion artifacts and other major technical restrictions- have constrained the application of these technologies in assessing CBF during motion sickness. To overcome this limitation, in this study we have adopted a standardized virtual reality (VR) provocation method to elicit motion sickness. Although motion sickness is characterized by a physical sensation of motion, exposure to VR provokes similar symptoms to motion sickness. This is caused by the feeling of movement in a virtual environment while being stationary. Cybersickness is relatively common, and most people feel some level of sickness during a provocative VR experience. A study on cybersickness symptoms discovered that 80% of subjects experienced symptoms of cybersickness in the first 10 minutes of their VR exposure [30]. In our previous studies where we used a simulated ride in a rollercoaster, with vigorous linear and angular accelerations, we found that all participants developed some level of nausea and/or other motion sickness symptoms during this provocative exposure [31, 32]. Some of the most common symptoms related to cybersickness were nausea, dizziness and disorientation that are similar to “classical” motion sickness symptoms.

The objective of this study was to examine temporal changes in cerebral blood flow in subjects who experience nausea during visually induced motion sickness. TCD and NIRS were used to study the changes in global and local CBF, respectively. To our knowledge these techniques have not been used to investigate brain hemodynamics during cybersickness. We hypothesized that blood flow would decrease in subjects who experience cybersickness symptoms. We also expected to see an increase in Posterior Cerebral Artery (PCA) blood flow due to activation of the visual cortex in response to visual provocation. We also anticipated that NIRS results would be consistent with TCD data, and will demonstrate a decrease in cortical blood flow in subjects who develop motion sickness.

2. METHODS

2.1. Participants

This study was conducted in two groups of young healthy subject with the approval of the Newcastle University Humans Research Ethics Committee. The exclusion criteria were history of vertigo, vestibular dysfunction or neurological disorders as well as ortostatic intolerance. All subjects verbally confirmed that they are healthy and not using any medication. Cerebral blood flow velocity was measured by trans-cranial Doppler (TCD) ultrasound in 14 volunteers (8 males and 6 females, average age 28±7.0 y.o. range 19-48 y.o.). Cortical blood flow was measured by functional near-infrared spectroscopy (fNIRS) in another group of 9 volunteers (4 male, 5 female, average age 33.3±5.4 y.o., range 26-42 y.o.)). All participants were exposed to visual provocations leading to motion sickness (visually-induced motion sickness, VIMS). All participants gave informed written consent and completed a Motion Sickness Susceptibility Questionnaire [33] before the experiment started.

2.2. Cerebral blood flow recordings

In the TCD monitoring experiment, after fitting a head-mounted VR display (Oculus Rift DK2, Oculus VR, USA), the 2 MHz TCD probes were placed bilaterally on the head and adjusted to obtain optimal flow signals from the MCA on one side and from the PCA on another side. The probes were connected to the TCD ultrasound device (DWL, Germany) that has a 100 Hz sampling rate.

The other group of participants were fitted with a skullcap containing 52-channel fiberoptic probes. We used an optical topography system (ETG-4000, Hitachi Medical Corporation, Japan) for the NIRS measurements. Designed for comfort and flexibility, the skullcap holds the sensors and detectors in place and secures the probes in precise locations around the subjects' head. The light source optical fiber tips are 'sprung', ensuring continual scalp contact for accurate readings. This device uses continuous laser diodes with two wavelengths, 695 and 830 nm, as light sources; the transmitted light signal is sampled every 100 ms.

2.3. Experimental setup, data collection and analysis

Before virtual ride commencement, a baseline 5-min recording was performed. During this period, a neutral static image was presented on the rift display. Subsequently, a simulated Helix rollercoaster ride (Helix, Archivision, Netherlands) was activated. The ride lasted for 15 min or until a subject decided to stop due to discomfort, whichever occurred first. During the experiment, subjective nausea ratings were assessed every minute using 10-point scale from zero (no nausea) to nine (just about to vomit). All recordings continued for 5 min after the ride termination. In the TCD study we also assessed heart rate (HR), systolic (SAP) and diastolic

(DAP) arterial pressure at the beginning and then every 2 minutes in the experiment using a cardiovascular profiling instrument PulseWave CR2000 (Hypertension Diagnosis, USA).

In the TCD experiment, systolic and diastolic TCD data were transferred into the Lab Chart 8.0 software (AD Instruments, Sydney, Australia) for analysis. As all participants terminated the ride at different times from the onset, overall averaging for their flow traces was not possible; thus, for comparison we selected two data points: "Baseline" (an average of the 2nd and 4th min of control period) and "End Ride" data from the last minute of the ride. Relative conductances of the MCA (C_{MCA}) and PCA (C_{PCA}) were computed according to the formula: $C_{MCA} = V_{MCA}/AP$ and $C_{PCA} = V_{PCA}/AP$, where V represents blood flow velocity in cm/s. Flow data values for these calculations were taken from 30 s before to 30 s after each AP and HR measurement. Statistical analyses were performed using Prism 7.0 (GraphPad, USA). Correlations between the subjective nausea ratings, ride duration and MSSQ score were assessed using Spearman's correlation. Paired t-tests were performed to determine the effect of cybersickness on HR, AP and MCA and PCA conductance. Two-way ANOVAs were performed to assess differences between time points and sex effects. Sex differences in ride duration, MSSQ and maximum nausea ratings were assessed using unpaired t-tests.

In the NIRS setting, digital data containing oxygenated haemoglobin (HbO_2), deoxygenated hemoglobin (deoxy-Hb) and total Hb values were transferred into Excel where initial analysis was performed. Our primary measure was oxy-Hb levels reflecting regional brain activity. Thirty seconds (300 samples) immediately prior to each subjective nausea rating were extracted and averaged for every channel. All 52 channels were analyzed individually for every subject. For the analysis of relationships between NIRS changes and nausea, data were grouped into "no nausea/baseline" (rating 0), "light nausea" (rating 1-3), "moderate nausea-strong" (rating 4-7) bins. Statistical analysis was performed using Prism 7 (GraphPad, USA). Sidak's multiple comparison one-way ANOVAs were performed to determine the effects of nausea on HbO_2 concentration. Correlations between the subjective nausea ratings, ride duration and MSSQ score were performed as described above. Data is presented as means ± standard error of the mean (S.E.M.). Differences between males and females were assessed by means of unpaired Student's t-test. Statistical significance was set at $p<0.05$.

3. RESULTS

3.1. TCD study.

The participants had a substantially varying MSSQ score ranging from zero to 29 (mean 13.7±3.7). No nausea was reported by any subject during the baseline recording. During the ride, all participants reported some level of nausea that gradually increased with time. Eleven

out of 14 participants terminated early (<15 min) due to discomfort. The average nausea rating in the last minute of the ride was 3.5±0.7; mean ride duration was 10±1.7 min.

There was a significant correlation (r^2= 0.38, p=0.01) between the subjective maximum nausea rating and MSSQ (Fig.1A), also a significant negative correlation was stablished (r^2=0.30, *p*=0.04) between the tolerated ride duration and MSSQ score (Fig 1B).

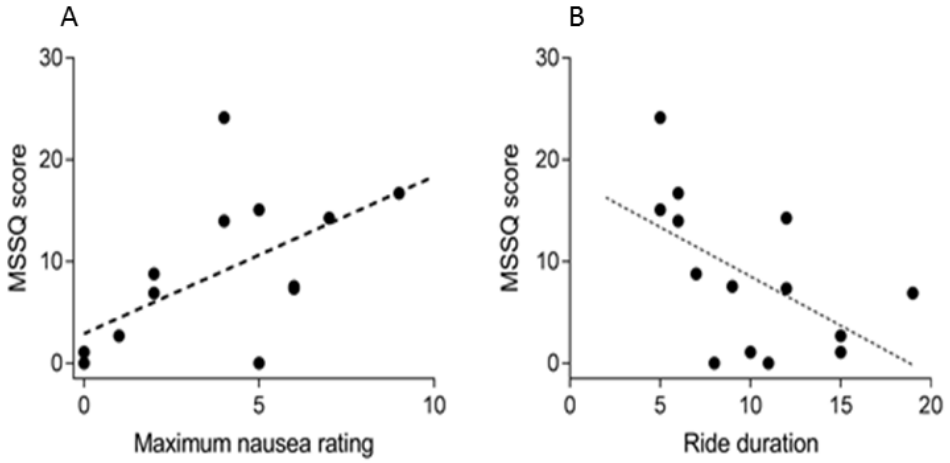

Fig 1. Relationship between MSSQ score and maximum nausea rating (A) correlation of tolerated ride time and MSSQ score (B). Dashed line shows result of linear regression.

There was a significant increase in heart rate (+5.8±2.4 bpm, t (13)=2.4, p=0.01) at the end of the ride compared to the baseline (77± 2.9 bpm, Fig 2A). SAP and DAP also significantly increased (+3.8±1.8 mmHg, *t*(13)=2.10, p= 0.02 and +6.7±1.3 mmHg , *t* (13)=4.95, p<0.001, respectively; Fig 2B and C) at the end of the ride when compared to baseline values (118.9±3.7 and 67±2.9 mmHg, respectively).

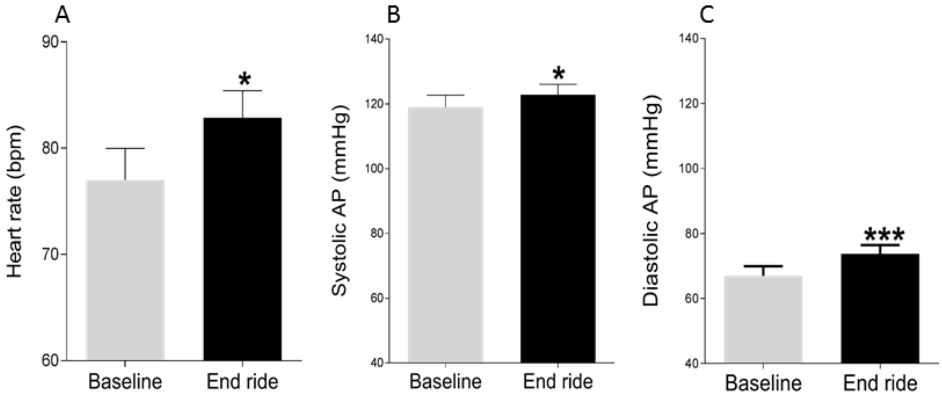

*Fig 2. Differences in HR (A), systolic arterial pressure (B) diastolic arterial pressure (C) between baseline and the last minute of the ride when nausea was maximal. * - p<0.05 compared to baseline; *** - 0.005 compared to baseline*

The PCA systolic flow velocity and conductance decreased significantly (- 5.15±2.42 cm/s, p=0.05 and-0.02±0.01cm x s^{-1} x $mmHg^{-1}$ p=0.03) at the end of the ride with maximum nausea when compared to baseline (Fig. 3A &B). PCA diastolic velocity and conductance did not did not show any significant change to baseline values at the end of the ride (Fig. 3 C&D).

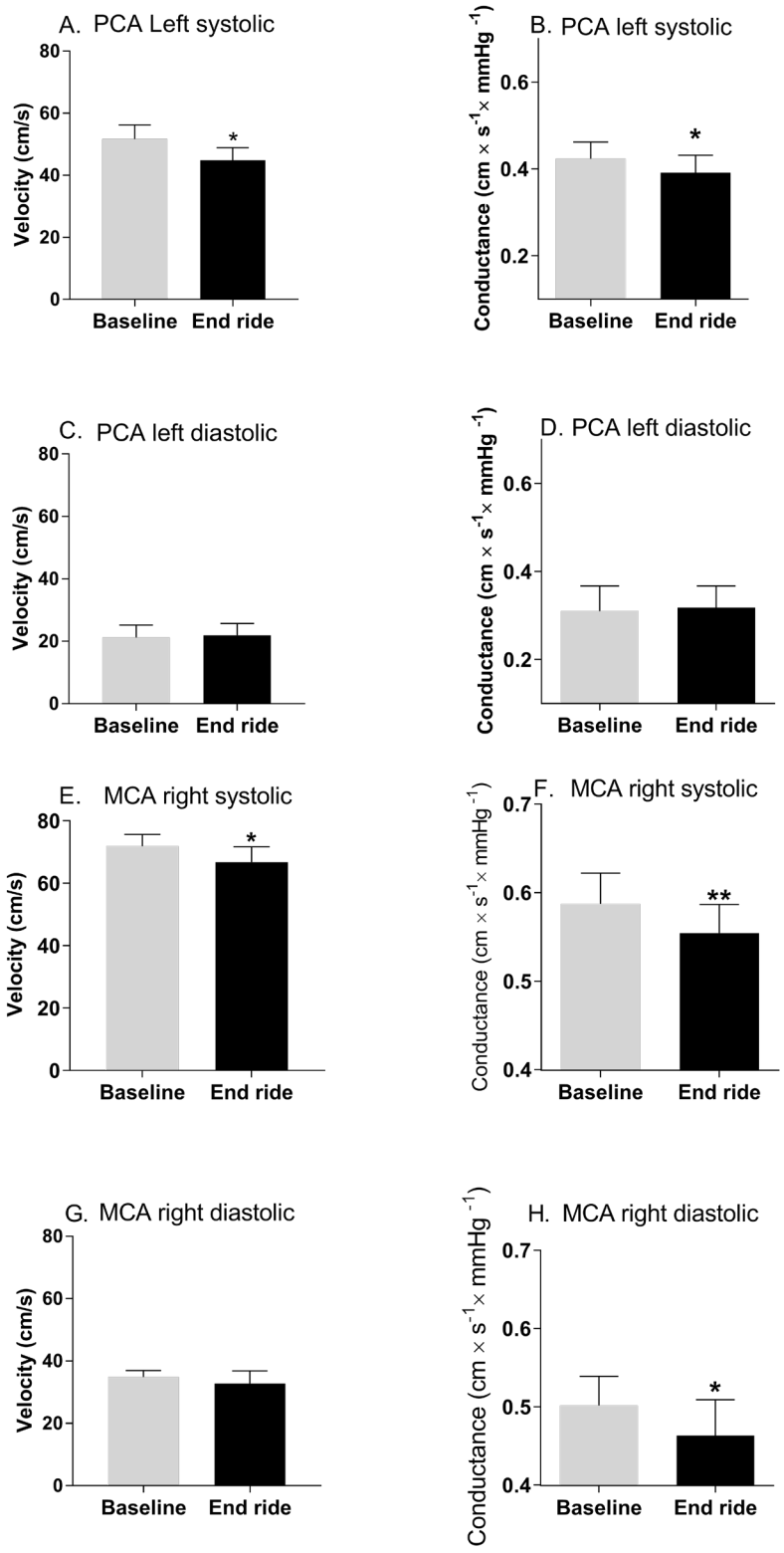

*Fig 3. Changes in velocity and conductance at baseline and the last minute of the ride (when nausea was maximal). A - PCA systolic velocity B - PCA systolic conductance, C- PCA diastolic velocity, D- PCA diastolic conductance, E- MCA systolic velocity, F- MCA systolic conductance, G- MCA diastolic velocity, H- MCA diastolic conductance. PCA velocity and conductance are measured from left side, MCA velocity and conductance are measured from the right side * - p<0.05, p < 0.001 compared to baseline.*

There was a significant decrease in MCA systolic velocity and conductance (- 5.15±2.42 cm/s, p=0.05 and -0.02±0.01cm x s^{-1} x $mmHg^{-1}$ p= 0.005, respectively) at the end of the ride when compared to the baseline, Fig. 3E&F. The diastolic MCA velocity remained unchanged (Fig. 3G). The diastolic MCA conductance decreased significantly (-0.03±0.01 cm x s^{-1} x $mmHg^{-1}$, p=0.05) in the end of the ride (Fig. 3H).

The increase in heart rate showed a significant positive correlation (r^2 = 0.51, p=0.005) with the reported nausea ratings (Fig. 4A). SAP level followed the same trend and a significant positive correlation (r^2 =0.43, p= 0.01) was stablished with subjective nausea ratings reported by the participants during the ride (Fig. 4B). Systolic MCA velocity showed a significant negative correlation (r= -0.36, p= 0.05) with nausea ratings (Fig. 4C).

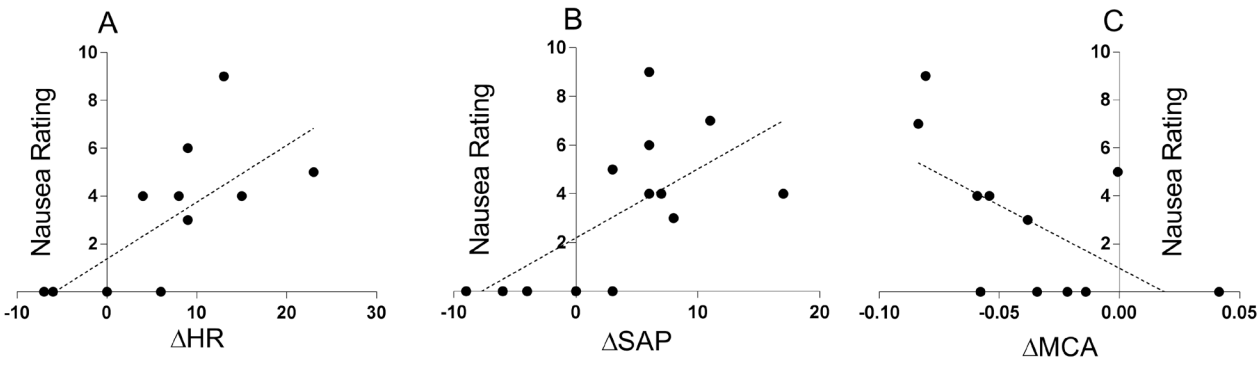

Fig. 4. Correlation between changes in Δ Heart-rate (A), ΔSAP (B), Δ MCA systolic velocity (C) and nausea ratings.

3.2. NIRS study

In the NIRS study, the MSSQ score varied significantly between subjects ranging from zero to 50 (mean 24.6±16.3). Nausea was not reported by any of the subjects during the baseline recordings. However, 8/9 subjects reported some level of nausea during the ride that gradually increased with time. Only one subject did not experience nausea or any form of motion sickness symptoms. This participant completed the 15-min ride designated for this experiment. The average nausea rating in the last minute of the ride was 4.8±2.2, and the mean ride duration was 7.5±1.7 min.

There was a significant positive correlation between the MSSQ score and maximal nausea level (r^2 = 0.58, p=0.01, Fig. 5A) and significant negative correlation between MSSQ score and ride duration (r^2 = 0.50, p = 0.03, Fig. 5B).

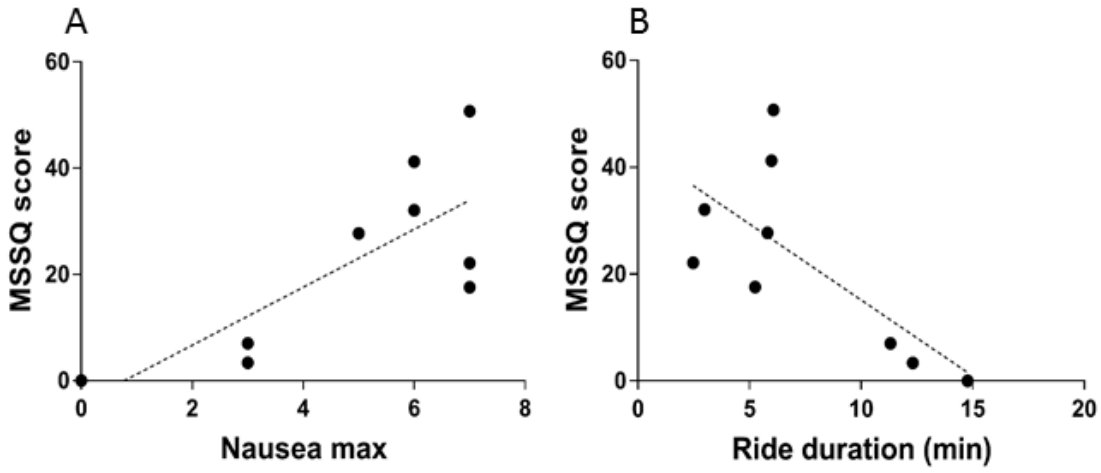

Fig 5. Relationship between MSSQ score and maximum nausea rating (A), tolerated ride duration and MSSQ (B)

Analysis of NIRS results revealed significant increases in HbO_2 concentration in parieto-temporal regions of both hemispheres in participants who experienced motion sickness symptoms during the experiment. These regions corresponded to 15/52 channels (eleven channels on the left hemisphere, four channels on the right hemisphere) as illustrated in Fig. 6A). There was no significant change in cortical HbO_2 concentration in one volunteer who did not experience nausea or any form of motion sickness symptoms

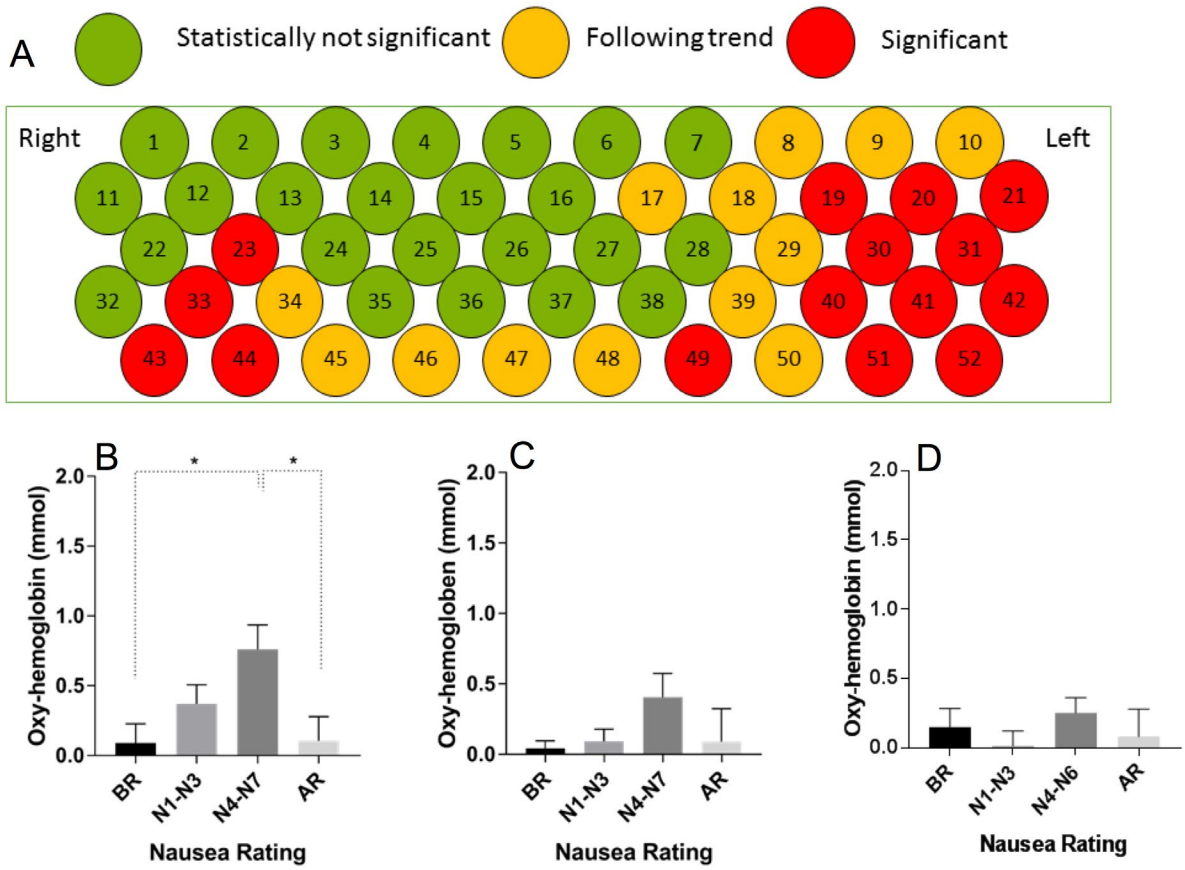

Fig 6. Changes in cortical blood flow induced by VR provocation. A - NIRS channel scheme demonstrating channels with significant changes in hemoglobin concentration (red), channels following the trend but not significant (orange), and channels without changes (green), B - Oxy-Hb concentration in channel 40 plotted against subjective nausea ratings during the VR roller coaster ride. C- Channel 45, D- channel 11. In B-D, data values are pooled for four conditions: before ride (BR), mild nausea (N1-N3), moderate/strong nausea (N4-N7) and after ride (AR).

In subjects who were susceptible to motion sickness, average oxy-hemoglobin concentration increased significantly with increasing subjective nausea ratings ($p=0.01$, $F(3, 35) = 3.79$). Group data for changes in HbO_2 for one of the "sensitive" channels (Ch 40) are presented in Fig 6B. Despite following the same trend, changes in HbO_2 concentration in 13/52 channels were not statistically significant (channels in orange color, Fig 6A); most of these channels were adjacent to "hot" channels. Group data for changes in HbO_2 for one of such channel (Ch 45) are shown in Fig 6C. As also could be seen in Fig 6A, the rest of the channels (24/52) did not show any correlation between the increasing nausea and perfusion in the cortex; they are shown in green; group data for changes in HbO_2 for one of such channel (Ch 11) are presented in Fig 6D.

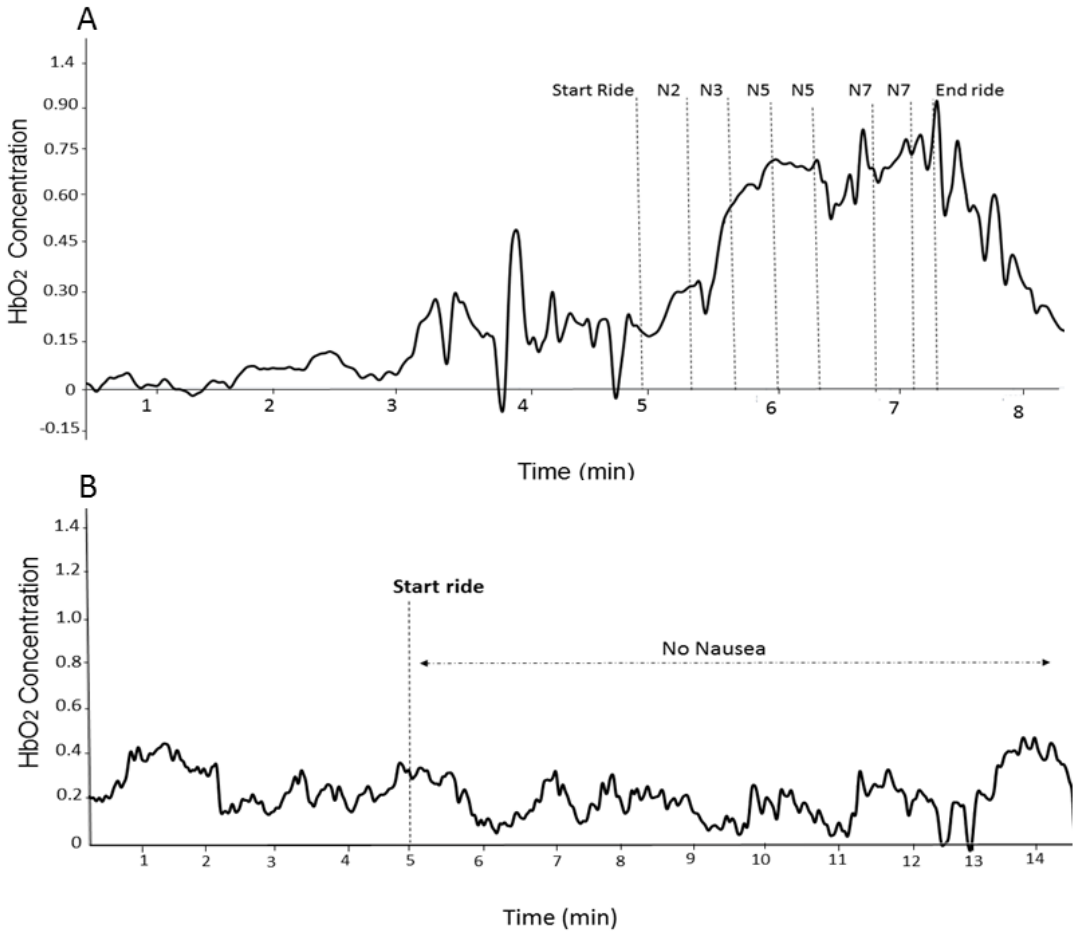

Fig 7. HbO_2 concentration from channel 40 during the VR provocation experiment in the subject with high level of nausea (panel A) and in the subject with no nausea (panel B). Note that in the susceptible subject, the HbO_2 value gradual increases with the onset of nausea, peaks at the time when nausea rating was maximal, and then gradually returns to the baseline. Vertical dashed lines depict ride onset/end and nausea (N) scores.

Two raw records of temporal changes in HbO_2 concentration are presented in Fig 7. The record shown in Panel A was obtained from Ch 40 in one of the susceptible individuals. It could be seen that HbO_2 gradually increased with the onset of nausea, and returned to the basal level within several minutes after ride termination. The record in Fig. 7B (also Ch 40) is from the subject who did not experience any nausea; in this case there were no changes in HbO_2 levels.

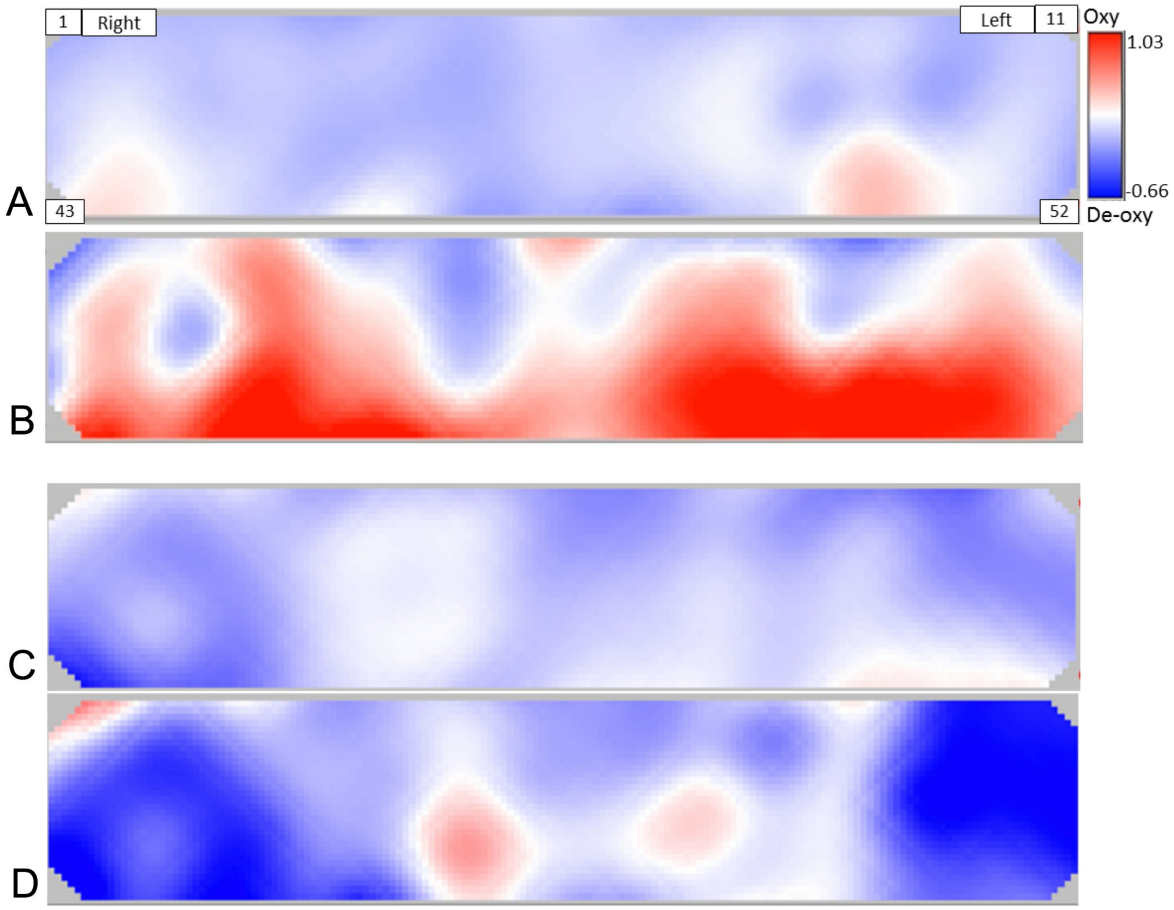

Fig 8. Changes in HbO_2 concentration during VR provocation in a susceptible subject (A-B) and in a resistant subject (C-D). The panels show 2D topographic images of NIRS signal before the ride onset (A,C) and at the highest level of nausea (B) or before ride termination (D). Inset – pseudo-color scale of HbO_2 concentration.

Two-dimensional topographic images of all the NIRS channels recorded during the VR experiment are displayed in Fig 8. The upper panels (A&B) illustrates dramatic changes in cortical blood flow in an individual who terminated his virtual ride at nausea level 7. The bottom panels (C&D) are from the subject who did not experience any nausea; his cerebral blood flow remained largely unchanged.

Table 1 presents spatial relationship between channels that were activated in our study and relevant cortical areas. The data are compiled based on the study Sato et al. [21] that employed identical channel setup. It could be seen that activated regions correspond mostly to the temporal, frontal and parietal lobes on the left side and to the temporal lobe on the right side.

Table 1. *Estimated location of each NIRS channel and corresponding Brodmann area (BA) numbers are shown for each channel.*

NIRS channel Left	*# BA Area*	*Brodmann Area*
19	44	inferior frontal gyrus (Pars opercularis)
20	1, 43	Primary Somatosensory Cortex- 43 Primary gustatory cortex
21	40	Supramarginal gyrus
30	6	Premotor cortex and Supplementary Motor Corte
31	2, 43	Primary Somatosensory Cortex, 43 Primary gustatory cortex
40	45	inferior frontal gyrus (Pars triangularis)
41	43	Primary gustatory cortex
42	22	Superior temporal gyrus Wernicke's area
49	10	Anterior prefrontal cortex
51	48, 38, 21	Retrosubicular area, Temporopolar area, Middle temporal gyrus
52	21	Middle temporal gyrus

NIRS channel Right	*# BA AREA*	*BRODMANN AREA*
23	6	Premotor cortex and Supplementary Motor Cortex
33	22 43	Superior temporal gyrus, Primary gustatory cortex
43	21 22	Middle temporal gyrus, Superior temporal gyrus Wernicke's area
44	38 48 21	Temporopolar area, Retrosubicular area, Middle temporal gyrus

3.3. Male vs. female differences.

When an overall analysis was preformed on combined results from both studies, a substantialy and significantly higher MSSQ score was found in female participants when compared to males (25.8±4 vs.10.4±2.6, respectively, p=0.009, Fig 9A). The second sex difference was significantly higher nausea rating in females compared to males just prior the termination of the ride (5.4±0.5 vs. 3±0.8, respectively, p=0.03, Fig. 9B). Finally, the tolerated ride duration

was significantly shorter in females compared to males (7.0±0.7 vs. 10.9±1.4 min, respectively; p= 0.03, Fig. 9C). Analysis of physiological data such as HR, SAP, DAP, NIRS Hb-O_2 did not show any significant difference between female and male participants.

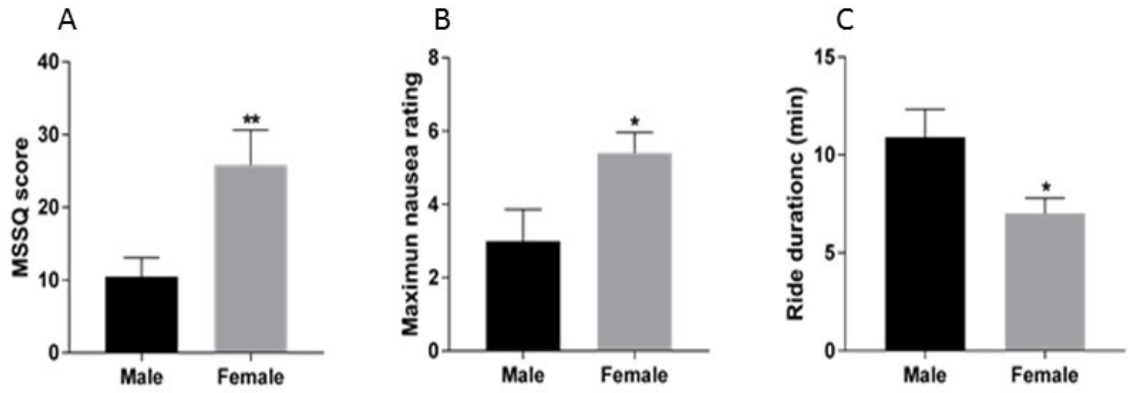

Fig 9. Diffrences between male and female participants in MSSQ score (A), maximum nausea rating (B) and tolerated ride duration (C).

4. DISCUSSION

The aim of the current study was to determine the effect of motion sickness on the brain blood flow during exposure to the provocative visual stimulation. In this regard, we used TCD ultrasonography to measure blood flow velocity in the two main cerebral arteries. Independent from the TCD setup, NIRS was used to monitor HbO_2 concentration during the same visual stimulation. In both experiments, nausea scores were recorded to monitor symptoms development. Of note, susceptibility and provocative effects of the virtual ride were very similar to those reported in our two previous studies where identical visual provocation was employed [31, 32].

This study provides two main findings. Firstly, we observed mild reduction in MCA and PCA conductance during motion sickness experience, suggesting vasoconstriction in downstream vascular beds supplied by the MCA and PCA in the TCD study. These changes were associated with mild increases in arterial pressure and heart rate. Importantly, the cardiovascular changes correlated with subjective nausea levels. Secondly, outcomes from the NIRS study showed apparent disaccord with the results in TCD study. When interpreting this discrepancy, in must be taken into account that the two methods assess different physiological variables – content of HbO reflecting blood supply to the cortical region (NIRS); or blood velocity in the two major cerebral arteries (TCD). Still, it is hard to reconcile substantial increases in cortical blood flow in brain areas responsible for balance and vestibular inputs in subjects who experienced nausea and motion sickness symptoms with modest generalized

decrease in cerebral blood flow in the same individuals. In the following discussion, we focus on these findings separately, and then try to explain the controversy.

Our TCD findings are in a good accord with a previous study by Serrador et al. who also found a decrease in cerebral blood flow velocity suggesting brain hypoperfusion during provocative motion (human centrifuge) [7]. Likewise, small but significant pressor responses were found in both experiments. These observations may suggest that reductions in cerebral blood flow are essential for the development of motion sickness. In the study by Serrador et al., the increase in cerebrovascular resistance has been linked to the autoregulatory response aiming to sustain a constant cerebral blood flow when there is an alteration in BP. The authors suggested that increases in BP result in vasoconstriction to preserve a relatively constant cerebral blood flow.
In the TCD study we also found small but significant increases in HR, systolic and diastolic arterial pressure after the onset of symptoms. These findings are consistent with our previous findings and other studies in this field [7, 31, 34]. While identifying a precise origin for the fluctuations is difficult, one possible cause of the autonomic changes could be due the general excitement/arousal associated with the onset of the virtual ride. In fact, in our previous study [32] we concluded that the increase in heart rate introduced during VIMS cybersickness is mostly associated with anxiety rather than with motion sickness *per se* and found that exposure to VIMS caused a significant decrease in cardiac vagal tone, which was associated with anxiety. Increases in anxiety ratings during VIMS have also been reported by Farmer et.al in a recent study on 98 healthy individuals [34], where he reported increased sympathetic and decreased parasympathetic tone, respectively, using cardio-metric indices.

Numerous functional studies have documented that an increase in HbO_2 concentration has been linked with cortical activation in specific regions of the brain [22, 23, 35]. Changes in cortical activity during motion sickness and nausea have been reported using functional magnetic source imaging [36], electroencephalography [37] and fMRI [38]. In this study we used NIRS to monitor cortical activation during VIMS which has previously been shown to have close correspondence to fMRI signals with significant spatial and temporal correlations [28] [29]. Analysis of the NIRS results show a significant increase in HbO_2 concentration in 15/52 channels of the NIRS device (Hitachi, ETG 4000). This increase in recorded HbO_2 concentration was correlated with increasing nausea and motion sickness symptoms (11/15 channels). According to a study by Sato et al. [21] investigating the correspondents of NIRS channels and Broadman regions [39] the activated channels correspond to 9 cortical Broadman regions as shown in Table 1.

When considering the functional aspect of these cortical regions, many of them have been linked to motion sickness, nausea or in general to the vestibular sensory processing. One of the regions where a significant increase in HbO_2 concentration has been recorded is the inferior frontal gyrus; this area has been previously linked to visually induced motion sickness [34]. The superior temporal gyrus (STG) and middle temporary gyrus (MTG), two other regions activated during VIMS, contain the primary auditory cortex, which is responsible for processing sounds, semantic control, and a region for processing multisensory integration. Previous studies have also linked inputs from a vestibular system origin to these regions [40, 41]. STG has also been linked with active balancing [42, 43]. Supra-marginal gyrus (SMG) was also activated in our study; this region located in the parietal lobe has been described in many studies as an important element for analysing vestibular inputs [41, 44, 45]. The importance of the supra-marginal gyrus (SMG) has also been demonstrated by trans-cranial magnetic stimulation and fMRI to play a role in proprioception and resolution of conflicting sensory information such as sensorimotor conflicts [46, 47]. SMG has also been shown to play an important role in balance and maintaining postural stability [42, 43].

The primary gustatory cortex (GC) was activated in both hemispheres (channels #20, #31, #33, #41), this structure is known for its role in perception of taste has also been linked to more general functions rather than working as the receptive field of peripheral taste receptor cells. The central gustatory pathways operates as a multisensory structure that is dedicated to assessing the significance of intra-oral stimuli. Among these functions is the ability of GC to combine taste information with the post-ingestive consequences that follow the consumption of food [48]. Therefore one can argue that the activation of the GC region can be linked to the common symptoms of stomach awareness and nausea in motion sickness.

The supplementary motor area which is directly related with movement and balance was also activated during the VIMS test in this study. This activation potentially could be linked to the body movements associated with the ride.

Interestingly, only one subject was not affected by the motion sickness provocation during the NIRS recording. This subject reported no nausea or any other motion sickness related symptoms which was consistent with his MSSQ score of zero. The subject tolerated the maximum duration of the ride and rated zero for motion sickness related symptoms. The NIRS results for this subject showed minimal or no activation of the aforementioned regions. This finding shows that the regions activated in subjects with motion sickness is not activated in the subject with no symptoms.

In summary, previous brain imaging studies reported changes in cortical activity during motion sickness [34, 36, 38, 49]. Overall there is a good accord in locations of activated areas between these studies and our experiments. However, there are some inconsistency in the activated areas described by Farmer et al. [34] who noted negative correlations between intensity of nausea and neural activation in regions such as tonsil, lingual gyrus, posterior cingulate cortex and also a positive correlation with the inferior frontal gyrus. These findings are in contrast with the study by Napadow [38], and the discrepancies could be potentially explained by the differences in the experimental protocol and the subject selection, and further confirm the complexity of mechanisms involved in developing motion sickness.

The most challenging question of the current discussion is how to reconcile contradicting results obtained by the two different methods. As already noted, our TCD results are in good agreement with two previous studies using the same method. One limitation of TCD is that it measures cerebral blood velocity rather than flow. In order for velocity variations to correspond to flow changes, the diameter of the artery must remain constant. In a study combining MRI and TCD, Serrador et al. confirmed that MCA diameter at the insonation point does not change during large fluctuations in cerebral flow velocity provoked by changes in end tidal CO_2 and lower body negative pressure [50]. So how can it be that a small global fall in cerebral blood flow is associated with regional cortical increases in HbO_2 concentration reflecting increases in local blood supply? The only possibility that we can propose to explain this puzzling observation is that with the development of nausea and other motion sickness symptoms, a complex re-balancing occurs in the brain hemodynamics, so that increases in blood supply in described cortical regions are potentially offset by decreases in deeper cortical and subcortical areas (such as hypothalamus, pons or medulla) that are not accessible to NIRS detection, and resulting in small global reduction in CBF. This alteration in blood flow results in increased perfusion in some critical regions responsible with balance (vestibular region) and deactivation of some other regions as described by Farmer et al. in his recent study using fMRI to image cortical activation during VIMS [34].

There was a substantial difference in susceptibility to cybersickness between the subjects. This was determined both by subjective and objective measures. Since one of our exclusion criteria was previous exposure to VR, these differences were clearly unrelated to this factor. However, it is not excluded that variations in symptoms were in part due to possible differences in head movements throughout the ride, and lack of considering this constraint is a study limitation. It is however implausible that the extent of head movements made a significant contribution to the sensory conflict, due to the very nature of the VR hardware and software that matched voluntary induced shifts in the virtual visual field due to head rotations and tilts,

thus preventing vestibulo-visual sensory mismatch. Therefore the actual interaction was between virtual linear and angular accelerations and lack of corresponding sensations from the vestibular receptors which resulted in a vestibulo-visual conflict.

We found that sensitivity to cybersickness is higher in females compared to males. This result is in accord with findings from other studies with visually induced motion sickness [51-53]. It is well established that females are also more sensitive to provocative motion stimuli [54, 55]; combined, these facts suggest that sex-related mechanisms exert their action via affecting central processing of relevant information rather than influence initial sensory processing. We did not find expected sex differences in physiological changes associated with cybersickness; one potential reason for this is a relatively small number of participants in our pilot study. The major argument in favour of this idea is that sex differences for nausea sensitivity reached the level of significance only when data were analysed from all participants together, but was insignificance when the data were analysed separately for TCD and NIRS groups.

In conclusion, considering earlier studies [34], [36, 38, 56] together with our results, we conclude that motion sickness in general and nausea in particular is associated with variations in brain activity (region-specific increases and decreases) in a complex pattern in numerous cortical regions related to the cognitive evaluative and sensory discriminative aspects of this syndrome [49]. The findings in this study can further emphasize the complexity of neural pathways during motion sickness and underline the importance of the vestibular system in developing motion sickness. Our results provide an incremental step towards resolving a fundamental question of identifying a neural substrate of motion sickness. From immediate practical perspective, our finding represent interest is in the field of occupational health rather than clinical settings. In a most recent pilot study we have confirmed that cortical flow is also elevated by motion-induced motion sickness. The latter is a major problem during pilot training, and providing reliable biomarker of nausea will be of major benefit here.

Acknowledgement: This work was supported by funding from the Australasian Society of Aerospace Medicine.

References

[1] Reason, J. Motion sickness / J. T. Reason, J. J. Brand. London ; New York: Academic Press; 1975.
[2] Irwin, J. A. The pathology of sea-sickness The Lancet. 1881,118:907-9.
[3] James, W. Sense of dizziness in deaf-mutes. Mind. 1881:412-3.
[4] Reason, J., Brand, J. Motion sickness. London: Academic Press; 1975.
[5] Johnson, W. H., Sunahara, F. A., Landolt, J. P. Importance of the vestibular system in visually induced nausea and self-vection. J Vestib Res. 1999,9:83-7.
[6] Serrador, J. M., Shoemaker, J. K., Brown, T. E., Kassam, M. S., Bondar, R. L., Schlegel, T. T. Cerebral vasoconstriction precedes orthostatic intolerance after parabolic flight. Brain Res Bull. 2000,53:113-20.
[7] Serrador, J. M., Schlegel, T. T., Black, F. O., Wood, S. J. Cerebral hypoperfusion precedes nausea during centrifugation. Aviat Space Environ Med. 2005,76:91-6.
[8] Heckmann, J. G., Leis, S., Muck-Weymann, M., Hilz, M. J., Neundorfer, B. Vestibular evoked blood flow response in the basilar artery. Acta Neurol Scand. 1999,100:12-7.
[9] Wallesch, C. W., Henriksen, L., Kornhuber, H. H., Paulson, O. B. Observations on regional cerebral blood flow in cortical and subcortical structures during language production in normal man. Brain Lang. 1985,25:224-33.
[10] Heiss, W. D., Herholz, K., Pawlik, G., Wagner, R., Weinhard, K. Positron emission tomography in neuropsychology. Neuropsychologia. 1986,24:141-9.
[11] Risberg, J. Regional cerebral blood flow in neuropsychology. Neuropsychologia. 1986,24:135-40.
[12] Mazzucco, S., Diomedi, M., Qureshi, A., Sainati, L., Padayachee, S. T. Transcranial Doppler screening for stroke risk in children with sickle cell disease: a systematic review. Int J Stroke. 2017,12:580-8.
[13] Purvis, D. L., Crutchfield, K., Trickey, A. W., Aldaghlas, T., Rizzo, A., Sikdar, S. Transcranial Doppler investigation of hemodynamic alterations associated with blunt cervical vascular injuries in trauma patients. J Ultrasound Med. 2013,32:1759-68.
[14] Guan, J., Zhou, Q., Ouyang, H., Zhang, S., Lu, Z. The diagnostic accuracy of TCD for intracranial arterial stenosis/occlusion in patients with acute ischemic stroke: the importance of time interval between detection of TCD and CTA. Neurol Res. 2013,35:930-6.
[15] Chilosi, A. M., Bulgheroni, S., Turi, M., Cristofani, P., Biagi, L., Erbetta, A., et al. Hemispheric language organization after congenital left brain lesions: A comparison between functional transcranial Doppler and functional MRI. J Neuropsychol. 2017.
[16] Ciambra, G., Arachi, S., Protano, C., Cellitti, R., Caoci, S., Di Biasi, C., et al. Accuracy of transcranial ultrasound in the detection of mild white matter lesions in newborns. Neuroradiol J. 2013,26:284-9.
[17] Droste, D. W., Harders, A. G., Rastogi, E. A transcranial Doppler study of blood flow velocity in the middle cerebral arteries performed at rest and during mental activities. Stroke. 1989,20:1005-11.
[18] Aaslid, R. Visually evoked dynamic blood flow response of the human cerebral circulation. Stroke. 1987,

18:771-5.
[19] Taussky, P., O'Neal, B., Daugherty, W. P., Luke, S., Thorpe, D., Pooley, R. A., et al. Validation of frontal near-infrared spectroscopy as noninvasive bedside monitoring for regional cerebral blood flow in brain-injured patients. Neurosurg Focus. 2012,32:E2.
[20] Causse, M., Chua, Z., Peysakhovich, V., Del Campo, N., Matton, N. Mental workload and neural efficiency quantified in the prefrontal cortex using fNIRS. Sci Rep. 2017,7:5222.
[21] Sato, H., Yahata, N., Funane, T., Takizawa, R., Katura, T., Atsumori, H., et al. A NIRS-fMRI investigation of prefrontal cortex activity during a working memory task. Neuroimage. 2013,83:158-73.

[22] Auger, H., Bherer, L., Boucher, E., Hoge, R., Lesage, F., Dehaes, M. Quantification of extra-cerebral and cerebral hemoglobin concentrations during physical exercise using time-domain near infrared spectroscopy. Biomed Opt Express. 2016,7:3826-42.
[23] Takehara, N., Tsubaki, A., Yamazaki, Y., Kanaya, C., Sato, D., Morishita, S., et al. Changes in Oxyhemoglobin Concentration in the Prefrontal Cortex and Primary Motor Cortex During Low- and Moderate-Intensity Exercise on a Cycle Ergometer. Adv Exp Med Biol. 2017,977:241-7.
[24] Metzger, F. G., Schopp, B., Haeussinger, F. B., Dehnen, K., Synofzik, M., Fallgatter, A. J., et al. Brain activation in frontotemporal and Alzheimer's dementia: a functional near-infrared spectroscopy study. Alzheimer's Research & Therapy. 2016,8:56.
[25] Takizawa, R., Kasai, K., Kawakubo, Y., Marumo, K., Kawasaki, S., Yamasue, H., et al. Reduced frontopolar activation during verbal fluency task in schizophrenia: a multi-channel near-infrared spectroscopy study. Schizophr Res. 2008,99:250-62.
[26] Wolf, M., Greisen, G. Advances in near-infrared spectroscopy to study the brain of the preterm and term neonate. Clin Perinatol. 2009,36:807-34, vi.
[27] Verhagen, E. A., Hummel, L. A., Bos, A. F., Kooi, E. M. W. Near-infrared spectroscopy to detect absence of cerebrovascular autoregulation in preterm infants. Clinical Neurophysiology.125:47-52.
[28] Huppert, T. J., Hoge, R. D., Diamond, S. G., Franceschini, M. A., Boas, D. A. A temporal comparison of BOLD, ASL, and NIRS hemodynamic responses to motor stimuli in adult humans. Neuroimage. 2006,29:368-82.
[29] Huppert, T. J., Hoge, R. D., Dale, A. M., Franceschini, M. A., Boas, D. A. Quantitative spatial comparison of diffuse optical imaging with blood oxygen level-dependent and arterial spin labeling-based functional magnetic resonance imaging. J Biomed Opt. 2006,11:064018.
[30] Cobb, S. V. G., Nichols, S., Ramsey, A., Wilson, J. R. Virtual Reality-Induced Symptoms and Effects (VRISE). Presence. 1999,8:169-86.
[31] Gavgani, A. M., Nesbitt, K. V., Blackmore, K. L., Nalivaiko, E. Profiling subjective symptoms and autonomic changes associated with cybersickness. Autonomic Neuroscience: Basic and Clinical.203:41-50.
[32] Mazloumi Gavgani, A., Hodgson, D. M., Nalivaiko, E. Effects of visual flow direction on signs and symptoms of cybersickness. PLoS One. 2017,12:e0182790.
[33] Golding, J. F. Motion sickness susceptibility questionnaire revised and its relationship to other forms of sickness. Brain Research Bulletin. 1998,47:507-16.
[34] Farmer, A. D., Ban, V. F., Coen, S. J., Sanger, G. J., Barker, G. J., Gresty, M. A., et al. Visually induced nausea causes characteristic changes in cerebral, autonomic and endocrine function in humans. J Physiol. 2015,593:1183-96.
[35] Hock, C., Villringer, K., Müller-Spahn, F., Wenzel, R., Heekeren, H., Schuh-Hofer, S., et al. Decrease in parietal cerebral hemoglobin oxygenation during performance of a verbal fluency task in patients with Alzheimer's disease monitored by means of near-infrared spectroscopy (NIRS) — correlation with simultaneous rCBF-PET measurements. Brain Research. 1997,755:293-303.
[36] Miller, A. D., Rowley, H. A., Roberts, T. P., Kucharczyk, J. Human cortical activity during vestibular- and drug-induced nausea detected using MSI. Ann N Y Acad Sci. 1996,781:670-2.
[37] Chelen, W. E., Kabrisky, M., Rogers, S. K. Spectral analysis of the electroencephalographic response to motion sickness. Aviat Space Environ Med. 1993,64:24-9.
[38] Napadow, V., Sheehan, J. D., Kim, J., Lacount, L. T., Park, K., Kaptchuk, T. J., et al. The brain circuitry underlying the temporal evolution of nausea in humans. Cereb Cortex. 2013,23:806-13.
[39] Jacobs, K. M. Brodmann's Areas of the Cortex. In: Kreutzer JS, DeLuca J, Caplan B, eds. Encyclopedia of Clinical Neuropsychology. New York, NY: Springer New York; 2011. p. 459-.
[40] Karim, H., Fuhrman, S. I., Sparto, P., Furman, J., Huppert, T. Functional brain imaging of multi-sensory vestibular processing during computerized dynamic posturography using near-infrared spectroscopy. Neuroimage. 2013,74:318-25.
[41] Dieterich, M., Bense, S., Lutz, S., Drzezga, A., Stephan, T., Bartenstein, P., et al. Dominance for vestibular cortical function in the non-dominant hemisphere. Cereb Cortex. 2003,13:994-1007.

[42] Mihara, M., Miyai, I., Hatakenaka, M., Kubota, K., Sakoda, S. Role of the prefrontal cortex in human balance control. Neuroimage. 2008,43:329-36.
[43] Ouchi, Y., Okada, H., Yoshikawa, E., Nobezawa, S., Futatsubashi, M. Brain activation during maintenance of standing postures in humans. Brain. 1999,122 (Pt 2):329-38.
[44] Fasold, O., von Brevern, M., Kuhberg, M., Ploner, C. J., Villringer, A., Lempert, T., et al. Human vestibular cortex as identified with caloric stimulation in functional magnetic resonance imaging. Neuroimage. 2002,17:1384-93.
[45] Stephan, T., Deutschlander, A., Nolte, A., Schneider, E., Wiesmann, M., Brandt, T., et al. Functional MRI of galvanic vestibular stimulation with alternating currents at different frequencies. Neuroimage. 2005,26:721-32.
[46] Tsakiris, M., Costantini, M., Haggard, P. The role of the right temporo-parietal junction in maintaining a coherent sense of one's body. Neuropsychologia. 2008,46:3014-8.
[47] Tsakiris, M., Longo, M. R., Haggard, P. Having a body versus moving your body: neural signatures of agency and body-ownership. Neuropsychologia. 2010,48:2740-9.
[48] de Araujo, I. E., Simon, S. A. The gustatory cortex and multisensory integration. International journal of obesity (2005). 2009,33:S34-S43.
[49] Stern, R. M., Koch, K. L., Andrews, P. Nausea: mechanisms and management: Oxford University Press; 2011.
[50] Serrador, J. M., Picot, P. A., Rutt, B. K., Shoemaker, J. K., Bondar, R. L. MRI measures of middle cerebral artery diameter in conscious humans during simulated orthostasis. Stroke. 2000,31:1672-8.
[51] Flanagan, M. B., May, J. G., Dobie, T. G. Sex differences in tolerance to visually-induced motion sickness. Aviat Space Environ Med. 2005,76:642-6.
[52] Munafo, J., Diedrick, M., Stoffregen, T. A. The virtual reality head-mounted display Oculus Rift induces motion sickness and is sexist in its effects. Exp Brain Res. 2017,235:889-901.
[53] Koslucher, F., Haaland, E., Malsch, A., Webeler, J., Stoffregen, T. A. Sex Differences in the Incidence of Motion Sickness Induced by Linear Visual Oscillation. Aerospace medicine and human performance. 2015,86:787-93.
[54] Dobie, T., McBride, D., Dobie, T., Jr., May, J. The effects of age and sex on susceptibility to motion sickness. Aviat Space Environ Med. 2001,72:13-20.
[55] Lawther, A., Griffin, M. J. A survey of the occurrence of motion sickness amongst passengers at sea. Aviat Space Environ Med. 1988,59:399-406.
[56] Kim, J., Napadow, V., Kuo, B., Barbieri, R. A combined HRV-fMRI approach to assess cortical control of cardiovagal modulation by motion sickness. Conf Proc IEEE Eng Med Biol Soc. 2011,2011:2825-8.